AMERICAN SOCIETY FOR MICROBIOLOGY | Journal of Bacteriology

The *Pseudomonas aeruginosa* PAO1 Two-Component Regulator CarSR Regulates Calcium Homeostasis and Calcium-Induced Virulence Factor Production through Its Regulatory Targets CarO and CarP

Manita Guragain,[a] Michelle M. King,[a] Kerry S. Williamson,[b] Ailyn C. Pérez-Osorio,[b]* Tatsuya Akiyama,[b] Sharmily Khanam,[a] Marianna A. Patrauchan,[a] Michael J. Franklin[b]

Department of Microbiology and Molecular Genetics, Oklahoma State University, Stillwater, Oklahoma, USA[a]; Department of Microbiology and Immunology, Montana State University, Bozeman, Montana, USA[b]

ABSTRACT

***Pseudomonas aeruginosa* is an opportunistic human pathogen that causes severe, life-threatening infections in patients with cystic fibrosis (CF), endocarditis, wounds, or artificial implants. During CF pulmonary infections, *P. aeruginosa* often encounters environments where the levels of calcium (Ca^{2+}) are elevated. Previously, we showed that *P. aeruginosa* responds to externally added Ca^{2+} through enhanced biofilm formation, increased production of several secreted virulence factors, and by developing a transient increase in the intracellular Ca^{2+} level, followed by its removal to the basal submicromolar level. However, the molecular mechanisms responsible for regulating Ca^{2+}-induced virulence factor production and Ca^{2+} homeostasis are not known. Here, we characterized the genome-wide transcriptional response of *P. aeruginosa* to elevated [Ca^{2+}] in both planktonic cultures and biofilms. Among the genes induced by $CaCl_2$ in strain PAO1 was an operon containing the two-component regulator PA2656-PA2657 (here called *carS* and *carR*), while the closely related two-component regulators *phoPQ* and *pmrAB* were repressed by $CaCl_2$ addition. To identify the regulatory targets of CarSR, we constructed a deletion mutant of *carR* and performed transcriptome analysis of the mutant strain at low and high [Ca^{2+}]. Among the genes regulated by CarSR in response to $CaCl_2$ are the predicted periplasmic OB-fold protein, PA0320 (here called *carO*), and the inner membrane-anchored five-bladed β-propeller protein, PA0327 (here called *carP*). Mutations in both *carO* and *carP* affected Ca^{2+} homeostasis, reducing the ability of *P. aeruginosa* to export excess Ca^{2+}. In addition, a mutation in *carP* had a pleotropic effect in a Ca^{2+}-dependent manner, altering swarming motility, pyocyanin production, and tobramycin sensitivity. Overall, the results indicate that the two-component system CarSR is responsible for sensing high levels of external Ca^{2+} and responding through its regulatory targets that modulate Ca^{2+} homeostasis, surface-associated motility, and the production of the virulence factor pyocyanin.**

IMPORTANCE

During infectious disease, *Pseudomonas aeruginosa* encounters environments with high calcium (Ca^{2+}) concentrations, yet the cells maintain intracellular Ca^{2+} at levels that are orders of magnitude less than that of the external environment. In addition, Ca^{2+} signals *P. aeruginosa* to induce the production of several virulence factors. Compared to eukaryotes, little is known about how bacteria maintain Ca^{2+} homeostasis or how Ca^{2+} acts as a signal. In this study, we identified a two-component regulatory system in *P. aeruginosa* PAO1, termed CarRS, that is induced at elevated Ca^{2+} levels. CarRS modulates Ca^{2+} signaling and Ca^{2+} homeostasis through its regulatory targets, CarO and CarP. The results demonstrate that *P. aeruginosa* uses a two-component regulatory system to sense external Ca^{2+} and relays that information for Ca^{2+}-dependent cellular processes.

Pseudomonas aeruginosa, a natural inhabitant of soil and water, is able to infect a variety of hosts, including plants and humans. In humans, it causes severe acute and chronic infections by colonizing respiratory and urinary tracts and burned or wounded epithelia, cornea, and muscles (1–3). The versatility of *P. aeruginosa* pathogenicity is associated with diverse metabolic capabilities, multiple mechanisms of resistance, a large repertoire of virulence factors, and adaptability, due in part to the tightly coordinated regulation of gene expression. A large portion of the *P. aeruginosa* PAO1 genome, approximately 9.4%, encodes transcriptional regulators (4, 5), including two-component regulators: 89 response regulators, 55 sensor kinases, and 14 sensor-response regulator hybrids (2). The regulatory targets for most of these regulatory systems are unknown.

Calcium plays an important signaling role in both eukaryotic and prokaryotic cells. In prokaryotes, Ca^{2+} is an essential nutrient, since it is a necessary cofactor for many enzymes. However, Ca^{2+} can be toxic to cells at high concentrations; therefore, bacteria maintain a low-submicromolar intracellular concentration of Ca^{2+} (6). *P. aeruginosa* may encounter environments where

Received 9 December 2015 **Accepted** 31 December 2015

Accepted manuscript posted online 11 January 2016

Citation Guragain M, King MM, Williamson KS, Pérez-Osorio AC, Akiyama T, Khanam S, Patrauchan MA, Franklin MJ. 2016. The *Pseudomonas aeruginosa* PAO1 two-component regulator CarSR regulates calcium homeostasis and calcium-induced virulence factor production through its regulatory targets CarO and CarP. J Bacteriol 198:951–963. doi:10.1128/JB.00963-15.

Editor: G. A. O'Toole, Geisel School of Medicine at Dartmouth

Address correspondence to Marianna A. Patrauchan, m.patrauchan@okstate.edu, or Michael J. Franklin, franklin@montana.edu.

* Present address: Ailyn C. Pérez-Osorio, Washington State Department of Health Public Health Laboratories, Shoreline, Washington, USA.

Supplemental material for this article may be found at http://dx.doi.org/10.1128/JB.00963-15.

external Ca^{2+} levels are in the millimolar range, varying from 10 mM in soil (7) to 40 mM in hypersaline lakes (8). As a plant and human pathogen, *P. aeruginosa* may be exposed to lower but also varying Ca^{2+} levels. For example, in plants, the Ca^{2+} concentration ranges from 0.01 to 1 mM in extracellular spaces (9) and from 1 to 10 mM in apoplasts (10). In a human body, Ca^{2+} levels may reach about 1 to 2 mM in extracellular fluids and saliva (11) (12) and 5 mM in blood (13) and human milk (14). In the case of disease, for example, during cystic fibrosis (CF) pulmonary infections, both intracellular and extracellular Ca^{2+} levels fluctuate in response to inflammation (15, 16), and the overall Ca^{2+} levels in nasal secretions and sputum increase at least 2-fold (12), reaching up to 3 to 7 mM (17, 18).

In a previous study, we demonstrated that *P. aeruginosa* maintains a submicromolar intracellular concentration of Ca^{2+} ($[Ca^{2+}]_{in}$) (6). However, when the cells are exposed to high levels of extracellular Ca^{2+}, characteristic of the environments described above, the cells undergo a transient increase of $[Ca^{2+}]_{in}$. The transient increase is followed by a return to submicromolar levels of $[Ca^{2+}]_{in}$ and a maintenance of homeostatic concentrations of internal Ca^{2+}, apparently due to the transport of excess Ca^{2+} through Ca^{2+} export pumps. Interestingly, in addition to the maintenance of Ca^{2+} homeostasis, *P. aeruginosa* recognizes the external concentration of Ca^{2+} as a physiological signal and responds through changes in the abundances of intracellular proteins and secreted virulence factors, alginate, pyocyanin, and secreted proteases (19, 20). This Ca^{2+}-triggered change in *P. aeruginosa* physiology leads to enhanced plant infectivity (21), biofilm formation, and swarming motility (6, 19, 20). Furthermore, Ca^{2+} alters the abundance of *P. aeruginosa* proteins involved in iron acquisition, quinolone signaling, nitrogen metabolism, and stress responses (19, 20). These observations suggest that Ca^{2+} plays an important regulatory role in *P. aeruginosa* virulence. However, the molecular mechanisms responsible for sensing environmental Ca^{2+} and regulating the Ca^{2+}-induced responses are not known. Therefore, the goals of this study were to identify and characterize Ca^{2+}-mediated molecular responses.

Bacteria use two-component regulatory systems (TCSs) to sense and respond to diverse and continuously changing environmental stimuli, including changing cation concentrations. TCSs help regulate responses to Na^{+}, Mg^{2+}, and other cations; therefore, they likely are involved in Ca^{2+}-dependent regulation. A typical TCS contains a sensor kinase located partially in the cytoplasmic membrane and a cognate response regulator (22). Upon exposure to a stimulus, the sensor kinase autophosphorylates at histidine residues. The consequent conformation change enables the transfer of a phosphate group to the aspartate residue on the cognate response regulator, which typically results in DNA binding to an activator DNA sequence and changes in gene expression (5, 23). *P. aeruginosa* has many TCSs, and some of these have been characterized. For example, PhoPQ and PmrAB regulate resistance to polymyxin B and antimicrobial peptides via lipid A modification at a low magnesium (Mg^{2+}) concentration (24–27). PhoPQ also regulates aminoglycoside resistance, twitching and swarming motility, surface attachment, and biofilm formation, ultimately contributing to the regulation of virulence (28, 29). PmrAB is induced by cationic antimicrobial peptides, including polymyxins (25), whereas PhoPQ is induced by polyamines and low $[Mg^{2+}]$ (30). Other TCSs respond to metals, including the CzcRS and CopRS systems that regulate resistance to zinc and copper, respectively (31, 32). CzcRS also regulates the transcription of the CzcrBCA resistance-nodulation-division (RND) efflux pump, which is responsible for carbapenem resistance (31). GacAS and AlgRZ regulate the production of several virulence factors, including pyocyanin, cyanide, lipase, and alginate, as well as systemic virulence and motility (29, 33–37). GacAS also controls the production of the quorum-sensing signaling molecule N-butyryl-homoserine lactone (38) and resistance to diverse antibiotics, including the aminoglycosides (such as gentamicin) and chloramphenicol (29). The transcription of *gacS* is repressed by subinhibitory concentrations of tobramycin, ciprofloxacin, and tetracycline (39). AlgRZ also regulates early stages of biofilm formation (40) and the expression of quorum-sensing genes (41). Another TCS, FleRS, regulates flagellar synthesis, adhesion (42), motility, and antibiotic resistance (43). Five TCS response regulators, PA1099, PA3702, PA4547, PA4493, and PA5261, are involved in coordinating the interactions of the bacterium with the host lung epithelium (44). However, most other TCSs on the *P. aeruginosa* genome remain uncharacterized, with their signals and regulatory targets yet to be identified.

In this study, we used microarray analysis to characterize the global transcriptional response of *P. aeruginosa* to elevated external Ca^{2+} levels. From these analyses, we identified the TCS PA2656-PA2657 (here referred to as *carSR*, for calcium regulator sensor and regulator), whose transcription is highly induced by elevated Ca^{2+} in planktonic cultures of *P. aeruginosa* PAO1. Using deletion mutations and microarray analysis, we identified the regulatory targets of *carSR*, which include the hypothetical proteins PA0320 and PA0327. Further characterization of PA0320 and PA0327 indicate that they play roles in maintaining Ca^{2+} homeostasis. PA0327 also influences the production of the virulence factor pyocyanin and swarming motility in a Ca^{2+}-dependent manner.

MATERIALS AND METHODS

Bacterial strains, plasmids, and media. Strains and plasmids used in this study are listed in Table S1 in the supplemental material. *P. aeruginosa* PAO1 is a nonmucoid strain with the complete genome sequence available (2). *P. aeruginosa* FRD1 is a mucoid cystic fibrosis isolate that also has an available genome (45) sequence. Isogenic mutants were constructed in PAO1. The gene PA2657 (*carR*) was deleted from PAO1 using allelic exchange as described previously (19). PAO1 mutants with transposon insertion in PA0320 (PA0320-H07::IS*lacZ*/hah) and PA0327 (PA0327-B11::IS*phoA*/hah) were provide by the University of Washington two-allele library. The sites of transposon insertions were confirmed by two-step PCR, using the primer sequences available at www.gs.washington.edu. For convenience, the transposon mutants were designated PA::Tn*5*, where PA is the identifying number of the disrupted gene from the *P. aeruginosa* PAO1 genome (www.pseudomonas.com). Each mutant gene was complemented by cloning the gene behind the arabinose-inducible P_{BAD} promoter in the Tn*7* vector pTJ1 (46) (graciously provided by Joanna Goldberg). For complementing vectors, PA0320 and PA0327 were amplified using PCR with the gene-specific primers listed in Table S1. The PCR products were cloned into TA cloning vectors (Invitrogen). The resulting plasmids were digested with NcoI and HindIII, and the bands containing PA0320 and PA0327 were ligated into pTJ1, producing plasmids pTA56 and pTA57, respectively. A Tn*7*-based construct containing both PA2657 and PA2656 was used to complement the PA2657 mutant to correct for any possible polar effects due to the disruption of PA2657. PA2656 and PA2657 were amplified separately using Phusion high-fidelity DNA polymerase (NEB). After the addition of a 3′ A overhang by *Taq* DNA polymerase, PCR products were cloned into TA cloning vectors. The

EcoRI-EcoRV fragment containing PA2656 was ligated into pTJ1, followed by ligation of the EcoRI fragment containing PA2657. The resulting plasmid was labeled pTA104. The Tn*7*-based vectors were integrated into the chromosome of the respective *P. aeruginosa* mutant strains using electroporation, along with the Tn*7* transposase helper plasmid, pTNS1, with selection for trimethoprim resistance. The trimethoprim resistance marker then was removed using pFLP2 (47). pTNS1 and pFLP2 were graciously provided by Herbert Schweizer.

For the estimation of free intracellular calcium ($[Ca^{2+}]_{in}$), PAO1 and mutant derivatives were transformed with pMMB66EH-AEQ (graciously provided by D. Dominguez and A. Campbell), which carries the gene for aequorin (48), and was selected for by carbenicillin resistance (49). The presence of the aequorin gene in the resulting strains was verified by PCR using the aequorin-specific primers (see Table S1 in the supplemental material).

Biofilm and planktonic cultures were cultivated in biofilm minimal medium (BMM) (19) which contained (per liter) 9.0 mM sodium glutamate, 50 mM glycerol, 0.02 mM $MgSO_4$, 0.15 mM NaH_2PO_4, 0.34 mM K_2HPO_4, 145 mM NaCl, 20 μl trace metals, and 1 ml vitamin solution. The trace-metal solution consisted of (per liter of 0.83 M HCl) 5.0 g $CuSO_4 \cdot 5H_2O$, 5.0 g $ZnSO_4 \cdot 7H_2O$, 5.0 g $FeSO_4 \cdot 7H_2O$, and 2.0 g $MnCl_2 \cdot 4H_2O$. Vitamins solution contained (per liter) 0.5 g thiamine and 1 mg biotin. The pH of the medium was adjusted to 7.0. When required, $CaCl_2 \cdot 2H_2O$ was added to a final concentration of 10 mM.

Growth of planktonic cultures and biofilms. *P. aeruginosa* strains PAO1 and FRD1 were cultured planktonically for 18 h at 37°C, with shaking at 250 rpm, in BMM with 10 mM added $CaCl_2$ or with no added $CaCl_2$. Biofilms were cultured on the surface of silicone tubing at 37°C in a single flowthrough system for 72 h with and without 10 mM added $CaCl_2$ as described previously (19). Biofilms were detached from the interior surface of the silicone tubing with the plunger from a 3-ml syringe. For FRD1, the cells were plunged into 150 ml of 110 mM sodium citrate. All resulting cell suspensions were collected by centrifugation at 10,000 rpm at 4°C for 3 min.

For physiological studies of PAO1 and its mutant derivatives, cells were cultured by inoculating 100 μl of a mid-exponential-phase culture into 100 ml of BMM alone or with 10 mM $CaCl_2$. Cultures were incubated at 37°C at 200 rpm with absorbance sampling every 2 to 4 h in a Biomate 3 spectrophotometer (Thermo Scientific).

RNA extraction, processing, and microarray analysis. RNA was isolated from cells using a hot phenol extraction method (50). Briefly, pelleted cells were suspended in 1.5 ml lysis buffer (0.15 M sucrose, 0.01 M sodium acetate, pH 4.5) and 1.5 ml 2% sodium dodecyl sulfate. Following the addition of 3 ml of water-saturated phenol, the mixture was incubated for 5 min at 65°C with frequent vortexing. Three milliliters of chloroform was added, and the mixture was centrifuged for 30 min at 4°C. The aqueous phase was precipitated overnight, washed, and resuspended in RNase-free water. The RNA was cleaned on an RNeasy column (Qiagen) by following the manufacturer's mini cleanup protocol and then subjected to two 30-min Turbo DNase (Ambion) treatments before precipitation and resuspension. RNA quality was assessed using an RNA6000 nano assay (Bioanalyzer 2100; Agilent Technologies, Palo Alto, CA). Labeled cDNA was synthesized from 8 μg of total RNA according to SOP#M007 (from the J. Craig Venter Institute [JCVI], formerly The Institute for Genomic Research [TIGR]), using a 2:1 ratio of amino-allyl dUTP to dTTP and Superscript II. cDNA quality and dye incorporation were assessed with a NanoDrop 1000.

Pseudomonas aeruginosa version 1 glass slide DNA microarrays were obtained from the JCVI and prepared according to SOP#M008, with minor modifications. For each condition (PAO1 planktonic, PAO1 biofilm, FRD1 planktonic, and FRD1 biofilm), labeled cDNA from cells grown with 10 mM added $CaCl_2$ and cells grown with no added $CaCl_2$ were cohybridized to the same slide, and a dye swap was performed. In this manner, for each of the four growth conditions, a minimum of four biological samples was hybridized to four microarrays.

Microarray slides were scanned using a GenePix 4000B scanner (Molecular Devices), and emissions at 532 and 650 nm were recorded. GenePix Pro software v 6.0 (Molecular Devices) was used to obtain median pixel intensity values for each spot on the array and generate GenePix Results (gpr) files. gpr files were imported into Flexarray v 1.6.1 for normalization and analysis. Background correction was performed using the normexp algorithm. The LOESS algorithm was used for within-array normalization, followed by scaling for between-array normalization. The Limma TREAT (*t* tests relative to a threshold) method was used to generate symmetrical fold changes to conservatively assess differential expression due to calcium addition. Empty and reserved spots were not included in the data set. Replicate spots (three per gene) were averaged, and genes with a greater than 2-fold change at $P < 0.05$ were selected for further analysis.

For validation of the JCVI microarray data, two additional biological replicates of PAO1 were grown planktonically with and without 10 mM added $CaCl_2$ as described above. Affymetrix microarrays were performed with these samples as described previously (51). Transcripts identified as upregulated in two-color arrays (JCVI) also were found to be upregulated on the Affymetrix platform, with 92% (33/36) being greater than 2-fold upregulated ($P < 10^{-14}$). Transcripts identified as downregulated in two-color arrays also were downregulated on the Affymetrix platform, with 90% (26/29) being greater than 2-fold ($P < 10^{-14}$).

RT-qPCR. At 6, 12, and 24 h, 1-ml aliquots of wild-type and Δ*carR* mutant cells were removed from a 25-ml volume of BMM (with or without 10 mM $CaCl_2$ added), pelleted, and frozen at −80°C. RNA was extracted with the hot phenol method, cleaned on RNA Clean & Concentrator-25 columns (Zymo Research), and turbo DNase treated (Ambion). One-step reverse transcription-quantitative PCR (RT-qPCR) was performed with the Rotor-Gene SYBR green RT-PCR kit (Qiagen) as described previously (52). Three biological replicates for each strain, time point, and Ca^{2+} level were assayed in triplicate using primers designed for the *acpP*, PA0320, and PA0327 transcripts (see Table S1 in the supplemental material). Negative controls lacking reverse transcriptase were performed with each of the 36 samples and revealed that samples were free from DNA contamination. RT-qPCR efficiencies, calculated from the slope of standard curves using Rotor-Gene software, were similar for *acpP* (1.06), PA0320 (0.97), and PAO327 (1.03), with $r^2 > 0.98$ for each. The Relative Expression Software Tool (REST) (53) was used to calculate mean fold changes of PA0320 (*carO*) and PA0327 (*carP*) transcripts due to the addition of 10 mM Ca^{2+} (compared to no added Ca^{2+}) using *acpP* as a normalizer. To determine if transcripts were significantly upregulated by Ca^{2+}, a nonparametric one-tailed Mann-Whitney test, assuming unequal variation, was performed using GraphPad Prism version 6.04 for Windows. This test also was used to determine if there was a significant increase in fold change due to Ca^{2+} addition between the wild-type strain PAO1 and the Δ*carR* mutant strain.

Measurement of $[Ca^{2+}]_{in}$. Luminescence measurements and the estimation of free cellular calcium concentrations ($[Ca^{2+}]_{in}$) were done as described previously (6), with slight modifications. Briefly, mid-log-phase cells were induced with IPTG (1 mM) for 2 h for apoaequorin production and then harvested by centrifugation at 6,000 × *g* for 5 min at 4°C. Aequorin was reconstituted by incubating the cells in the presence of 2.5 μM coelenterazine for 30 min. One hundred microliters of cells with reconstituted aequorin were equilibrated for 10 min in the dark at room temperature. Luminescence was measured using a Synergy Mx multimode microplate reader (Biotek). To estimate the basal level of $[Ca^{2+}]_{in}$, the measurements were recorded for 1 min at 5-s intervals, the cells were challenged with 1 mM Ca^{2+} and mixed for 1 s, and then the luminescence was recorded for 20 min at 5-s intervals. The injection of buffer alone was used as a negative control and did not cause any significant fluctuations in $[Ca^{2+}]_{in}$. $[Ca^{2+}]_{in}$ was calculated by using the formula $pCa = 0.612 (-\log_{10}k) + 3.745$, where k is a rate constant for luminescence decay (per second) (54). The results were normalized against the total amount of available aequorin as described previously (6). The discharge was per-

formed by permeabilizing cells with 2% Nonidet 40 (NP-40) in the presence of 12.5 mM $CaCl_2$. The luminescence released during the discharge was monitored for 10 min at 5-s intervals. The estimated remaining available aequorin was at least 10% of the total amount of aequorin. The experimental conditions reported here were optimized to prevent any significant cell lysis.

Swarming motility assay. Swarming motility was assayed as described in reference 6. PAO1 and mutants were grown in 5 ml BMM with no added or 10 mM $CaCl_2$. Two microliters of the mid-log cultures normalized to an optical density at 600 nm (OD_{600}) of 0.3 were spot inoculated onto the surface of BM2 agar plates (62 mM potassium phosphate buffer [pH 7], 0.02 mM $MgSO_4$, 10 μM $FeSO_4$, 0.4% [wt/vol] glucose, 0.5% [wt/vol] Casamino Acids, and 0.5% [wt/vol] Difco agar) (34). After inoculation, the plates were incubated for 24 h, and then the colony diameters and morphology were recorded.

Pyocyanin analysis. Pyocyanin production was assayed by using chloroform extraction as described previously (21), with modifications. Briefly, *P. aeruginosa* cultures grown in BMM until late log phase were normalized to an OD_{600} of 0.3. Two microliters of the normalized culture was inoculated in the middle of a BM2 agar plate (34) and incubated for 24 h at 37°C. Since swarming colonies spread within agar matrix, they were excised from the agar and split in halves, one to be used for pyocyanin extraction and the other for total cellular protein quantification. Agar slices of the same size were used as negative controls. The samples were mashed into fine pieces. Pyocyanin was extracted with 30 ml chloroform followed by 15 ml of 0.2N HCl. The absorbance of the extract was measured at 520 nm, and the amount of pyocyanin was calculated by using a coefficient of extinction of 17.1 M^{-1} cm^{-1} (55) and normalized per milligram of total cell protein. The latter was determined by using the Bradford assay (EMD) by following the manufacturer's protocol. The data shown represent one of three independent experiments, each including three biological replicates. Statistical significance was calculated using Student's *t* test.

Antibiotic susceptibility assays. Antibiotic susceptibility assays were performed using tobramycin and polymyxin B E-strips (bioMérieux). In brief, strains were cultured in BMM with no added $CaCl_2$ or 10 mM $CaCl_2$ for 18 h and normalized to an OD_{600} of 0.1. One hundred microliters of the normalized cultures then was spread on BMM agar plates with or without added $CaCl_2$. E-strips with tobramycin and polymyxin B gradients were placed onto the inoculated plates. After 24 h of incubation at 37°C, the MICs were recorded by determining the concentration of antibiotics on the strip at which no bacterial growth was detected. At least three replicates were tested in at least two independent experiments; the reported MICs are the mean values of the collected measurements. The coefficient of variation between biological replicates was less than 25%.

Bioinformatics analyses. Sequence homology searches were performed using the NCBI nr database (GenBank release 160.1). Sequence alignments and phylogenetic analysis of histidine kinases and response regulators were performed using MEGA software (56). Homologous proteins were selected based on at least 25% identity over the full length of amino acid sequence. Functional domains were predicted using Pfam (57). Protein subcellular localization was predicted using pSORTb v3.0 (58) and Loc tree (59) analysis. Predictions of transmembrane helices and signal peptides were performed using TMHMM (60) and SignalP 4.0, respectively (61). Protein three-dimensional (3D) structure was predicted using HHpred (62) and iTASSER (63) and visualized using PyMOL (version 1.7.6; Schrödinger, LLC).

Microarray data accession number. The microarray data have been deposited in NCBI's Gene Expression Omnibus (64) and are accessible through GEO Series accession number GSE74491.

RESULTS

Transcriptome response of *P. aeruginosa* to Ca^{2+}. We performed whole-genome transcriptome analysis of *P. aeruginosa* strain PAO1 and the mucoid cystic fibrosis strain FRD1 in order to identify *P. aeruginosa* genes whose transcription is positively or negatively regulated by Ca^{2+}. The strains were cultured under low and high $CaCl_2$ concentrations (no added or 10 mM added $CaCl_2$) in both planktonic cultures and in biofilms. As with our prior proteomics results (20), the transcriptomics data showed both strain- and condition-specific effects on gene expression due to added Ca^{2+}. Table 1 shows genes differentially regulated by Ca^{2+} (at least 2-fold change in expression and $P < 0.05$) for strain PAO1 and the same genes in strain FRD1. Among the genes upregulated by Ca^{2+} in PAO1 is the operon PA0102-PA0104, encoding a carbonic anhydrase and permease that likely are involved in CO_2-mediated calcification (M. A. Patrauchan, unpublished data). The upregulated genes also included PA0320 and PA0327, encoding hypothetical proteins, whose role in calcium-dependent processes is described below. Also significantly upregulated by Ca^{2+} are the genes involved in quorum sensing, *lasI* and *rhlR*, as well as several genes that are regulated by the quorum-sensing systems. The latter include *hcnA*, encoding hydrogen cyanide production, and many of the *pvd* genes responsible for pyoverdine biosynthesis. Pyoverdine biosynthetic proteins were shown to increase in abundance in response to Ca^{2+} in our prior proteomics study (20).

Ca^{2+} influences the expression of three TCSs, *carSR*, *phoPQ*, and *pmrAB*. The expression of the novel TCS PA2656-PA2657 (here termed *carSR*) increased 10- to 12-fold in response to Ca^{2+}, while the TCSs *phoPQ* and *pmrAB* had significantly reduced expression (Table 1). The *carSR* operon contains four genes, which include the histidine kinase, *carS*, and the response regulator, *carR*, as well as two small periplasmic lipoproteins (PA2658 and PA2659), that both contain peptidase propeptide domains with possible protease inhibitory function. The increased expression of this operon was observed during the growth of PAO1 in planktonic culture but not in biofilms or in FRD1 cultures. The expression of both *phoPQ* and *pmrAB* TCSs was downregulated by Ca^{2+} in planktonic and biofilm cultures of both PAO1 and FRD1 (Table 1). Other studies have shown that PhoPQ affects the expression of the *arn* operon (PA3552-PA3559), which is involved in the modification of lipopolysaccharide (LPS) and enhanced resistance to cationic peptide antibiotics (28, 65). The transcriptomics results here are consistent with those results and indicate that Ca^{2+} also caused the reduced expression of the *arn* operon in biofilm and planktonic cultures of both PAO1 and FRD1 (Table 1).

P. aeruginosa encodes multiple TCSs from each of the OmpR, NarL, and NtrC subgroups. We performed a sequence alignment of paralogs from each of the TCS clades for both the histidine kinases and the response regulators. The results of the OmpR subclade for the response regulators are shown in Fig. 1. Interestingly, although having regulatory responses opposite those of Ca^{2+}, CarSR, PhoPQ, and PmrAB are closely related paralogs within the OmpR group, and all are involved in divalent cation sensing and osmoregulation (24).

CarSR regulates PA0320 and PA0327 in a Ca^{2+}-dependent manner. To identify the regulatory targets of CarSR, we constructed a deletion mutation of the *carR* response regulator in strain PAO1 and performed transcriptome analysis of the mutant strain grown at low and high $CaCl_2$ concentrations. The results were compared to the responses of wild-type strain PAO1 to Ca^{2+}. The expression of PA0320 and PA0327, which was highly upregulated by Ca^{2+} in the PAO1 strain, was unaffected by Ca^{2+} in the Δ*carR* mutant strain, suggesting that CarSR directly (or indirectly) regulates the transcription of PA0320 and PA0327 in a

TABLE 1 *P. aeruginosa* PAO1 genes affected by high calcium levels

PA no. and regulation status	Gene or domain	Change in growth between 0 and 10 mM $CaCl_2$ conditions for strain: PAO1 Planktonic Fold change	PAO1 Planktonic *P* value	PAO1 Biofilm Fold change	PAO1 Biofilm *P* value	FRD1 Planktonic Fold change	FRD1 Planktonic *P* value	FRD1 Biofilm Fold change	FRD1 Biofilm *P* value
Upregulated by high Ca during growth in planktonic culture									
PA0102	Carbonic anhydrase	7.1	<0.01	1.0	1.00	−1.1	1.00	−1.3	0.91
PA0103	Permease	5.6	<0.01	1.1	0.98	1.1	0.98	−1.5	0.83
PA0104	Hypothetical	3.5	0.03	1.3	0.91	−1.3	1.00	−1.0	1.00
PA0122	*rahU*	6.0	0.02	1.6	0.74	2.1	0.28	−2.6	0.26
PA0320	OB-fold	17.1	<0.01	1.0	1.00	1.3	0.96	1.8	0.69
PAO327	Ca^{2+}-binding β-propeller	13.0	<0.01	1.0	1.00	−1.0	1.00	1.0	1.00
PA0940	DUF2024	10.6	<0.01	1.2	0.97	−1.3	1.00	1.1	1.00
PA0941	Thioredoxin	10.3	<0.01	1.4	0.89	−1.3	1.00	1.3	0.99
PA0942	DNA binding	2.9	0.04	1.0	1.00	−1.3	0.99	−1.2	1.00
PA1134	DUF393	3.0	0.02	1.9	0.58	−1.2	1.00	1.2	0.99
PA1432	*lasI*	3.1	0.01	1.0	1.00	−1.9	0.54	−1.2	0.97
PA2081	*kynB*	3.3	0.02	1.0	1.00	−2.1	0.34	1.1	1.00
PA2193	*hcnA*	2.4	0.04	1.0	1.00	−1.8	0.72	−1.4	0.89
PA2384	Fur-like	3.1	0.02	2.1	0.32	1.0	1.00	1.1	1.00
PA2386	*pvdA*	4.1	<0.01	2.0	0.49	−1.3	0.99	1.1	1.00
PA2397	*pvdE*	2.6	0.02	2.2	0.29	1.1	1.00	−1.2	1.00
PA2412	Pyoverdine synthesis	7.6	<0.01	1.9	0.54	−1.1	1.00	1.4	1.00
PA2413	*pvdH*	3.4	<0.01	1.4	0.98	−1.0	1.00	1.1	1.00
PA2424	*pvdL*	2.6	0.03	2.2	0.35	−1.3	0.94	1.8	0.74
PA2425	*pvdG*	4.0	<0.01	2.3	0.21	−1.5	0.92	1.5	0.99
PA2427	Hypothetical	3.8	<0.01	1.4	0.89	−1.1	1.00	1.7	0.77
PA2656	Histidine kinase	9.7	<0.01	−1.1	1.00	1.1	1.00	1.1	1.00
PA2657	Response regulator	12.6	<0.01	−1.5	0.89	1.0	1.00	1.1	1.00
PA2658	PepSY domain	12.1	<0.01	−1.0	1.00	1.1	1.00	1.4	0.98
PA2659	PepSY domain	12.4	<0.01	−1.1	1.00	−1.2	1.00	−1.1	1.00
PA3322	DNA binding	2.8	0.03	1.0	1.00	−1.0	1.00	1.0	1.00
PA3407	*hasAp*	4.2	<0.01	1.1	1.00	1.1	1.00	−1.2	0.99
PA3477	*rhlR*	4.4	0.04	2.0	0.50	1.3	1.00	−1.8	0.79
PA3478	*rhlB*	6.9	0.04	2.1	0.47	1.2	1.00	−1.7	0.81
PA3885	*tpbA*	7.1	<0.01	−1.0	1.00	4.3	0.07	2.4	0.16
PA4141	Hypothetical	3.7	0.03	2.4	0.30	2.1	0.41	−1.4	0.94
PA4378	*inaA*	3.1	0.02	−1.3	0.99	2.7	0.05	1.4	0.93
PA4379	Hypothetical	5.1	<0.01	−1.6	0.83	3.8	<0.01	1.9	0.65
PA4469	Hypothetical	2.9	0.02	2.8	0.08	1.1	0.89	1.3	1.00
PA4517	DUF1705	5.0	0.01	1.1	1.00	15.0	<0.01	1.1	1.00
PA5530	Permease	5.7	<0.01	−1.4	0.79	4.6	<0.01	1.3	1.00
Upregulated by calcium during growth in biofilms, PA4570	Hypothetical	1.0	1.00	4.3	0.01	−2.0	0.37	−1.0	1.00
Downregulated by high Ca during planktonic growth									
PA0391	Hypothetical	−2.6	0.02	−1.2	0.95	−1.3	0.96	−3.7	0.01
PA0603	Transporter	−2.5	0.03	−1.0	1.00	−2.6	0.05	−1.1	1.00
PA0610	*ptrN*	−4.3	0.03	−1.9	0.56	−1.3	1.00	−2.0	0.48
PA0733	Pseudouridine synthase	−3.5	0.01	1.0	1.00	1.1	1.00	1.1	1.00
PA0865	*hpd*	−6.5	<0.01	−1.4	0.86	1.6	0.89	−1.2	0.98
PA1336	Histidine kinase	−4.2	<0.01	1.2	1.00	1.1	1.00	1.1	1.00
PA1541	Efflux transporter	−2.6	0.03	1.1	1.00	−1.1	1.00	1.3	0.98
PA1559	Epimerase	−3.0	0.01	−2.0	0.45	−16.6	<0.01	−13.1	<0.01
PA2780	DNA binding	−2.7	0.01	1.1	0.99	1.2	0.99	−1.4	0.94
PA3217	*cyaB*	−2.6	0.03	−1.4	0.76	1.0	1.00	−1.0	1.00
PA4555	*pilY2*	−4.8	0.02	1.3	0.98	1.0	1.00	−1.6	0.90
PA4556	*pilE*	−3.8	0.01	1.2	0.95	1.1	1.00	−1.5	0.92

(Continued on following page)

TABLE 1 (Continued)

PA no. and regulation status	Gene or domain	Change in growth between 0 and 10 mM $CaCl_2$ conditions for strain: PAO1 Planktonic Fold change	PAO1 Planktonic *P* value	PAO1 Biofilm Fold change	PAO1 Biofilm *P* value	FRD1 Planktonic Fold change	FRD1 Planktonic *P* value	FRD1 Biofilm Fold change	FRD1 Biofilm *P* value
PA4568	*rpmA*	−2.6	0.04	−1.1	1.00	1.3	1.00	1.3	0.99
PA4699	TPR domain	−2.5	0.03	−1.1	1.00	−1.0	1.00	1.3	0.99
PA4823	Hypothetical	−3.3	0.02	−1.2	1.00	−1.4	0.90	1.2	0.99
PA5024	Permease	−2.5	0.02	1.3	0.98	1.0	1.00	1.2	0.99
Downregulated by high Ca during biofilm growth									
PA0316	*serA*	1.3	1.00	−3.1	<0.01	1.0	1.00	−1.4	0.97
PA0890	*aotM*	1.5	0.98	−4.0	0.01	−5.2	<0.01	−5.6	<0.01
PA1053	Hypothetical	−1.4	0.90	−3.2	<0.01	6.7	0.12	−3.0	0.02
PA1927	*metE*	−1.1	1.00	−10.6	<0.01	−23.0	<0.01	−1.5	0.73
PA4453	ABC transporter	1.1	1.00	−2.6	0.03	−1.1	1.00	−1.9	0.65
PA4455	ABC transporter	−1.1	1.00	−3.0	0.03	−1.1	1.00	−1.9	0.65
PA4773	decarboxylase	−1.8	0.72	−9.1	0.01	−27.6	<0.01	−23.1	<0.01
PA4774	Spermidine biosynthesis	−2.3	0.28	−12.3	<0.01	−42.9	<0.01	−37.4	<0.01
PA4775	Hypothetical	−1.2	1.00	−4.9	0.01	−10.0	<0.01	−13.8	<0.01
PA4776	*pmrA*	−1.3	1.00	−4.3	0.02	−7.4	<0.01	−9.4	<0.01
PA4777	*pmrB*	1.1	1.00	−6.9	<0.01	−5.6	<0.01	−12.5	<0.01
PA4781	Response regulator	−1.9	1.00	−3.0	0.03	−1.5	0.98	−2.2	0.14
PA4782	Hypothetical	−2.7	0.19	−12.0	<0.01	−11.6	<0.01	−23.4	<0.01
PA4826	Hypothetical	−1.1	0.94	−4.7	0.01	−4.9	0.01	−1.3	0.99
Downregulated by high Ca during both planktonic and biofilm growth									
PA1178	*oprH*	−58.8	<0.01	−28.2	<0.01	−1.5	0.89	−12.8	0.04
PA1179	*phoP*	−15.1	<0.01	−18.1	<0.01	−1.3	0.98	−11.6	<0.01
PA1180	*phoQ*	−12.5	<0.01	−14.7	<0.01	−1.4	0.96	−11.2	<0.01
PA1343	Hypothetical	−12.2	<0.01	−13.5	<0.01	5.5	<0.01	−6.3	0.07
PA3552	*arnB*	−12.5	<0.01	−4.8	<0.01	−5.2	<0.01	−20.3	<0.01
PA3553	*arnC*	−11.1	<0.01	−4.7	<0.01	−8.3	<0.01	−29.4	<0.01
PA3554	*arnA*	−11.5	<0.01	−6.5	0.02	−27.5	<0.01	−43.5	<0.01
PA3556	*arnT*	−5.6	0.01	−5.1	0.01	−22.8	<0.01	−37.1	<0.01
PA3559	*arnG*	−5.2	0.02	−5.9	0.01	−5.9	0.04	−14.4	0.01
PA4010	Glycosylase	−4.7	<0.01	−4.3	0.01	−2.9	0.10	−4.7	<0.01
PA4011	Hypothetical	−3.5	0.02	−4.1	0.01	−3.2	0.11	−5.1	<0.01
PA4359	Transport	−4.2	<0.01	−3.8	0.01	−4.1	0.01	−11.5	<0.01
PA4825	*mgtA*	−4.0	0.05	−3.5	0.12	−3.7	0.06	−1.2	0.95

Ca^{2+}-dependent manner. To confirm the role of CarSR in the regulation of PA0320 and PA0327, we performed RT-qPCR on PAO1 and on the PAO1 Δ*carR* mutant using PA0320- and PA0327-specific primers. The results show that at the 6-h time point, PA0320 and PA0327 were slightly repressed by Ca^{2+} in both strains (Fig. 2A and B). However, after 12 and 24 h of growth, the expression of both PA0320 and PA0327 was induced by Ca^{2+} in strain PAO1 but not in the Δ*carR* mutant. PA0320 had a 4.5-fold increase in mRNA abundance due to Ca^{2+} at 24 h ($P = 0.05$) and PA0327 had a 4.1-fold increase due to Ca^{2+} ($P = 0.05$), as determined by a Mann-Whitney test. In the Δ*carR* mutant strain, PA0320 and PA0327 mRNA was slightly reduced by Ca^{2+}, confirming the role of *carR* in the Ca^{2+}-dependent transcription of PA0320 and PA0327.

Predicted roles of PA0320 and PA0327 based on protein structural models. Structural modeling of PA0320 using HHpred and iTASSER indicates that this protein contains an OB-fold (oligonucleotide/oligosaccharide binding motif) (see Fig. S1A and B in the supplemental material) with similarity to YgiW of *Escherichia coli* (66), which is required for cell survival in hydrogen peroxide and cadmium (67). PA0320 is predicted to have a signal peptide for transport of the protein to the periplasm. The 3D structure of PA0327, predicted by HHPred and I-Tasser, forms a 5-bladed β-propeller (see Fig. S1C and D). Structural homologs of PA0327 included YjiK, hemagglutinin-neuraminidase, α-L-arabinofuranosidases, and levansucrase, the latter two of which require Ca^{2+} for stability (reviewed in reference 68). The predicted SdiA-regulated domain is commonly found in TolB proteins, which include Ca^{2+}-dependent phosphotriesterases. Sequence analysis predicts that the N terminus of PA0327 has an uncleaved transmembrane domain, suggesting that PA0327 is anchored in the cytoplasmic membrane with the rest of the protein facing the

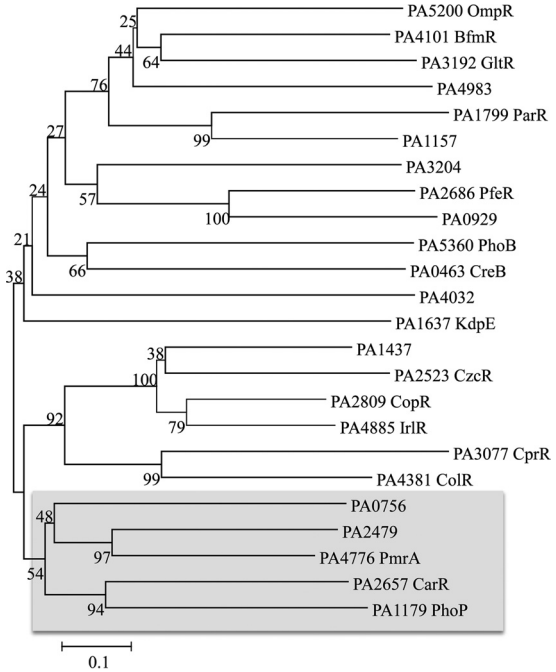

FIG 1 Phylogenetic analysis of *P. aeruginosa* response regulators in the OmpR clade of two-component systems. The OmpR response regulator protein sequences were aligned using MEGA software (56). Phylogenetic relationships were constructed by using neighbor-joining and bootstrapping analysis within the MEGA program. The shaded region shows the subclade that includes PhoP, PmrA, and CarR.

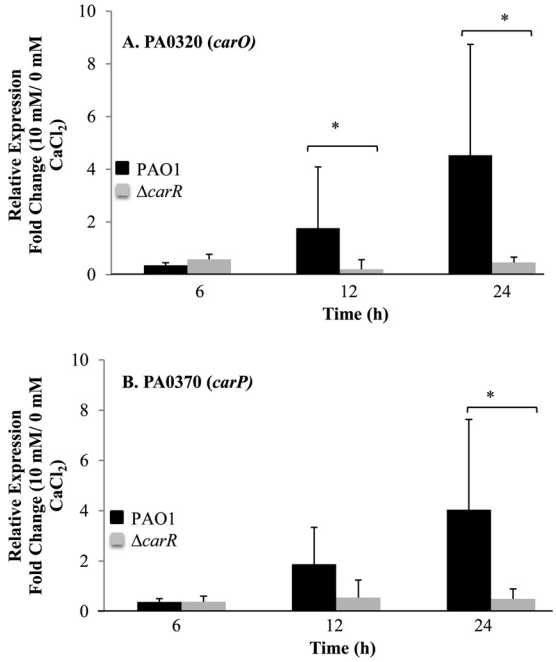

FIG 2 RT-qPCR analysis of PA0320 (*carO*) and PA0327 (*carP*) in *P. aeruginosa* PAO1 and in the *P. aeruginosa* Δ*carR* mutant. (A) Relative expression of *carO* in BMM with 10 mM $CaCl_2$ compared to that with 0 mM $CaCl_2$ for *P. aeruginosa* PAO1 and the *P. aeruginosa* Δ*carR* mutant. (B) Relative expression of *carP* in BMM with 10 mM $CaCl_2$ compared to that with 0 mM $CaCl_2$ for *P. aeruginosa* PAO1 and the *P. aeruginosa* Δ*carR* mutant. Data show the means and standard deviations for three biological replicates (three technical replicates for each biological replicate) at each time point. Asterisks represent a significant difference (at $P = 0.05$) in fold change, as determined by a Mann-Whitney test.

periplasm. Overall, the predicted structure of PA0327 suggests that it binds Ca^{2+} in a central pocket, and that Ca^{2+} binding is required for protein stability. PAO1 possesses two paralogs of PA0327 (PA0319 and PA2017) with 38 to 47% amino acid sequence identity. However, the expression of PA0319 and PA2017 is not affected by Ca^{2+}. Therefore, although PA0319 is adjacent to and in the same orientation as PA0320, these two genes have different regulatory mechanisms. From the structural predictions, we refer to PA0320 as CarO (for calcium-regulated OB-fold protein) and PA0327 as CarP (for calcium-regulated β-propeller protein).

CarP is required for optimal growth of PAO1 in high [Ca^{2+}] medium. In order to characterize the functional roles of *carO* and *carP* in response to Ca^{2+}, we obtained transposon mutants of each gene from the University of Washington two-allele library (69). Each mutation was complemented by cloning the respective gene into the single-copy Tn*7* expression vector pTJ1 (46). To determine the effect of Ca^{2+} on growth, each mutant strain and its respective complemented counterpart was cultured in BMM with or without 10 mM $CaCl_2$. The mutations in *carR* and *carO* did not affect growth at either Ca^{2+} level (Fig. 3). However, the *carP* mutation caused a defect in growth at high [Ca^{2+}]. The lag phase of the *carP*::Tn*5* mutant increased by 4 h, and the strain had a 2-fold decrease in growth rate. The maximum growth yield of the *carP*::Tn*5* mutant also was reduced in the presence of 10 mM $CaCl_2$. No effect on growth was observed for the *carP*::Tn*5* mutant when no Ca^{2+} was added to the medium. Complementation of *carP* restored the wild-type growth characteristics (Fig. 3).

CarSR regulates Ca^{2+} homeostasis in PAO1 through the activities of CarO and CarP. To characterize further the functional roles of CarRS and its regulatory targets, *carO* and *carP*, we measured the intracellular concentration of Ca^{2+} ($[Ca^{2+}]_{in}$) and monitored its changes in response to a rapid increase in extracellular $CaCl_2$. For this, we expressed the recombinant Ca^{2+}-binding luminescence protein, aequorin, in PAO1 and in its corresponding mutant strains. We assayed each strain when first cultured without $CaCl_2$ or with 10 mM $CaCl_2$. In the former case, PAO1 maintained $[Ca^{2+}]_{in}$ at 0.14 ± 0.05 μM, which transiently increased in response to the addition of 1 mM $CaCl_2$ (Fig. 4A to C, black lines) (6). Mutation in *carR* or *carO* did not affect the basal level of $[Ca^{2+}]_{in}$. The increase in the level of $[Ca^{2+}]_{in}$ following the addition of 1 mM $CaCl_2$ also was unaffected by the mutations (Fig. 4A and B, gray lines). However, the ensuing recovery to the resting $[Ca^{2+}]_{in}$ was impaired, and the remaining level of $[Ca^{2+}]_{in}$ was 6-fold higher in the Δ*carR* strain (Fig. 4A) and 2-fold higher in the *carO*:Tn*5* strain (Fig. 4B) than in wild-type PAO1, suggesting that CarR and CarO play roles in maintaining $[Ca^{2+}]_{in}$ homeostasis. Unlike the Δ*carR* and *carO*::Tn*5* mutants, the *carP*::Tn*5* strain had a 2.5-fold higher basal level of $[Ca^{2+}]_{in}$ (0.34 ± 0.17 μM) than PAO1 (Fig. 4C, inset). Recovery to the resting $[Ca^{2+}]_{in}$ from an immediate increase in response to external Ca^{2+} also was impaired, and the level of $Ca^{2+}{}_{in}$ remained 2.5-fold higher in the *carP*::Tn*5* strain (Fig. 4C, gray lines) than in PAO1 (Fig. 4C, black lines).

The intracellular Ca^{2+} levels also were measured when the strains first were cultured with 10 mM $CaCl_2$. For these experi-

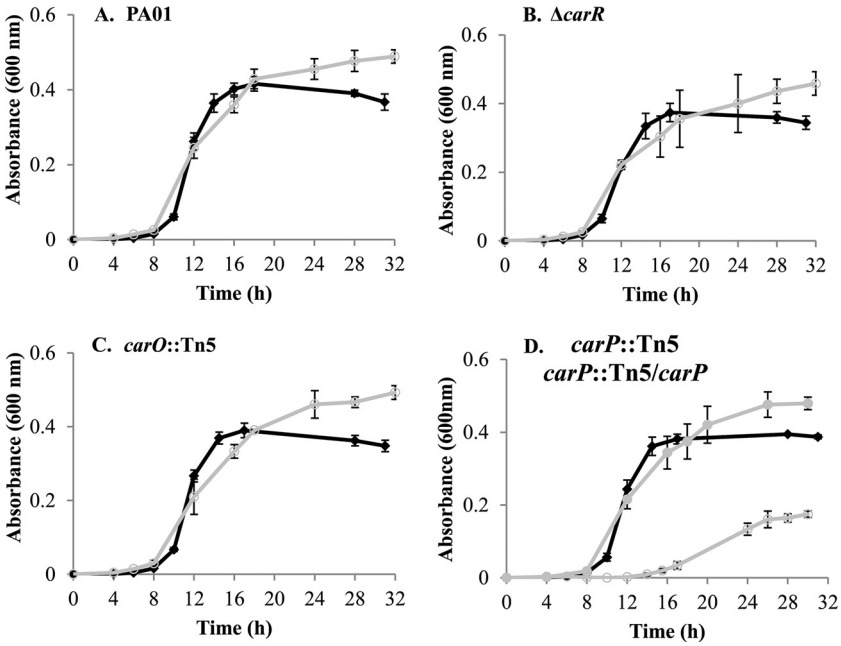

FIG 3 Growth of *P. aeruginosa* PAO1 and mutant strains in BMM containing 0 mM $CaCl_2$ (black diamonds) or 10 mM $CaCl_2$ (open gray circles). (A) Growth of *P. aeruginosa* PAO1 in BMM. (B) Growth of *P. aeruginosa* Δ*carR* mutant. (C) Growth of *P. aeruginosa carO*::Tn*5* mutant. (D) Growth of *P. aeruginosa carP*::Tn*5* mutant. Filled gray circles show the *P. aeruginosa carP*::Tn*5* mutant complemented with *carP*. Data show the means and standard deviations for three biological replicates.

ments, cells first were cultured in BMM with 10 mM $CaCl_2$, washed to remove excess $CaCl_2$, and assayed for response to the rapid addition of 1 mM Ca^{2+}. Under these conditions, the basal $[Ca^{2+}]_{in}$ for the wild-type strain was 0.35 ± 0.09 μM, or 2.5-fold higher than that when cultured in BMM without Ca^{2+} (Fig. 4D to F, black lines). The addition of 1 mM external Ca^{2+} resulted in increased $[Ca^{2+}]_{in}$ to 1.38 ± 0.03 μM and only partial recovery of resting $[Ca^{2+}]_{in}$ after 4 min, followed by a slow increase to 2.17 ± 0.48 μM after 20 min (Fig. 4D, black line). Mutation in *carR* or *carO* did not significantly change the $[Ca^{2+}]_{in}$ profile compared to that of the wild-type strain, with both strains showing partial recovery of the resting $[Ca^{2+}]_{in}$ at 4 min, followed by a slow increase in $[Ca^{2+}]_{in}$ (Fig. 4D and E, gray lines). However, the *carP*::Tn*5* mutant strain had a very different response to externally added Ca^{2+} (Fig. 4F, gray lines). First, the basal level of $[Ca^{2+}]_{in}$ was 3-fold higher than that in PAO1, at 0.98 ± 0.16 μM (Fig. 4F, inset). Second, recovery to basal levels following the addition of 1 mM $CaCl_2$ was impaired compared to that of the wild type, and the $[Ca^{2+}]_{in}$ remained elevated. The results indicate that $[Ca^{2+}]_{in}$ homeostasis was impaired in all three mutant strains when grown at low $[Ca^{2+}]$ and was impaired in the *carP*::Tn*5* mutant strain when first cultured with high $[Ca^{2+}]$.

CarP modulates Ca^{2+}-induced swarming motility and pyocyanin production. In previous work, we noted that Ca^{2+} addition results in phenotypic changes to *P. aeruginosa* (6). In particular, growth at elevated Ca^{2+} results in changes in swarming motility and pyocyanin production in the wild-type strain. The transcriptome data presented here show that elevated Ca^{2+} also causes an increase in the expression of genes for pyocyanin production (Table 1). Therefore, to determine if *carR*, *carO*, or *carP* plays a role in either of these Ca^{2+}-dependent phenotypes, we assayed the mutant and complemented strains for swarming motility and pyocyanin production at low and high Ca^{2+} levels. As seen in the prior study (6), 10 mM Ca^{2+} caused a 5-fold increase in PAO1 swarming (Fig. 5A and B). Mutation of *carR* or *carO* did not have a significant effect on swarming motility at any Ca^{2+} level (Fig. 5C to F). In contrast, the mutation in *carP* significantly altered the morphology of swarming colonies at elevated $[Ca^{2+}]$, showing multiple branches that extended from the swarming colonies (Fig. 5G and H). The complementation of *carP* restored the wild-type swarming morphology (Fig. 5I).

While the Δ*carR* and *carO*::Tn*5* mutants had pigment production similar to that of PAO1 at both low and high Ca^{2+} levels, the *carP*::Tn*5* mutant appeared impaired for pigment production in swarming colonies. We extracted and quantified pyocyanin produced by the swarming colonies. Figure 6 shows that the Tn*5* disruption of *carP* reduced the pyocyanin amount by 72%. The *carP* complemented strain had levels of pyocyanin production that were similar to those of the wild type.

***carO* and *carP* mutations cause increased sensitivity to tobramycin at high $[Ca^{2+}]$.** Our earlier studies showed that growth at elevated Ca^{2+} increases the MIC of PAO1 to tobramycin and polymyxin B (S. Khanam, D. L. Lenaburg, R. Kubat, and M. A. Patrauchan, unpublished data). To assess the potential role of *carR*, *carO*, and *carP* in Ca^{2+}-dependent resistance, we assayed each mutant and complemented strain for MIC using Etest strips (Fig. 7). In wild-type cells, the MIC for tobramycin was 8-fold greater in cells cultured at elevated Ca^{2+} levels. Both *carO*::Tn*5* and *carP*::Tn*5* strains had 2-fold reductions in tobramycin MIC when grown at elevated Ca^{2+} levels. The MIC for tobramycin was restored in these strains to the wild-type levels when the mutant genes were complemented. No difference in tobramycin susceptibility was detected in the *carO*::Tn*5* and *carP*::Tn*5* mutant cells cultured at low Ca^{2+} levels. The Δ*carR* mutation did not affect

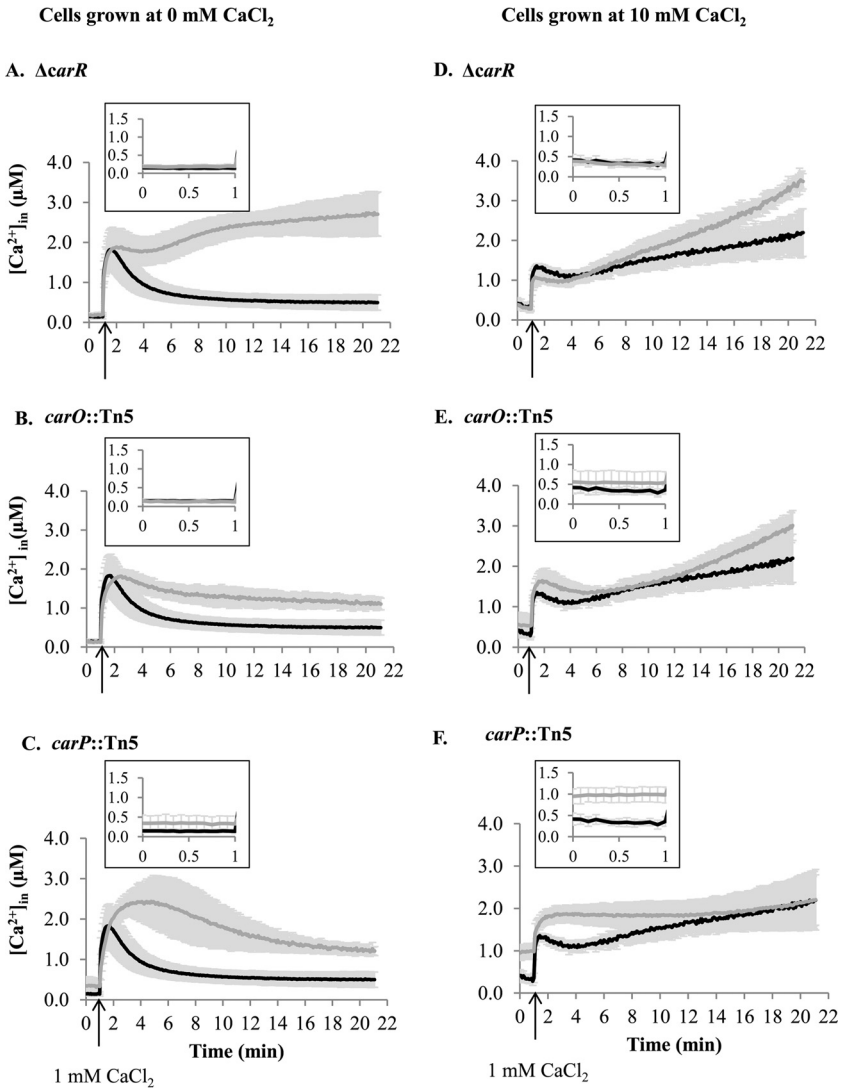

FIG 4 Free $[Ca^{2+}]_{in}$ profiles of *P. aeruginosa* wild-type strain PAO1 (black lines) and Δ*carR* (A and D), *carO*::Tn*5* (B and E), and *carP*::Tn*5* (C and F) mutants (gray lines). Cells were grown in BMM with 0 mM $CaCl_2$ (A, B, and C) or 10 mM $CaCl_2$ (D, E, and F). $CaCl_2$ (1 mM) was added at the time indicated by the arrow. Changes in free $[Ca^{2+}]_{in}$ were calculated as described in Materials and Methods. Insets show the basal level of $[Ca^{2+}]_{in}$ monitored for 1 min before 1 mM Ca^{2+} was added. Data show the means and standard deviations for at least three biological replicates.

tobramycin resistance at any Ca^{2+} level. The MIC of polymyxin B is 32-fold greater for the wild-type strain PAO1 when cells are cultured in the presence of 10 mM $CaCl_2$ than when no $CaCl_2$ is added to the medium. The mutations in *carR*, *carO*, or *carP* had no effect on polymyxin B resistance compared to that of the wild type at either Ca^{2+} concentration.

DISCUSSION

Our earlier studies showed that Ca^{2+} regulates a number of physiological processes, including virulence, in the opportunistic pathogen *P. aeruginosa* (6, 19–21). However, the molecular mechanisms responsible for sensing extracellular Ca^{2+} and orchestrating the cellular responses are not known. Here, we applied a genome-wide transcriptome analysis of *P. aeruginosa* to identify genes whose transcription is differentially regulated by Ca^{2+}. Among the genes identified as being induced by Ca^{2+} is an operon (PA2656-2659) containing the two-component regulatory system *carSR*. The CarSR proteins are closely related to other *P. aeruginosa* TCSs, PhoPQ and PmrAB, which are involved in Mg^{2+} sensing (24). Other Gram-negative bacteria have been shown to recognize or respond to extracellular Ca^{2+} through TCSs. In *Salmonella enterica* serovar Typhimurium, the PhoQ kinase of the PhoPQ system binds Ca^{2+}, Mg^{2+}, and Mn^{2+} and regulates the transcription of genes, including virulence factors (reviewed in reference 70). PhoQ has distinct Ca^{2+} and Mg^{2+} binding sites (71), suggesting an intricate nature of PhoPQ regulation by divalent cations. In *Vibrio cholerae*, the expression of the CarSR TCS negatively regulates polysaccharide production and biofilm formation in response to elevated Ca^{2+} (72). In *Escherichia coli*, AtoSC is induced by Ca^{2+} and regulates the biosynthesis and the intracellular distribution of cPHB [complexed poly-(R)-3-hydroxybutyrate], building the nonproteinaceous complexes that act as voltage-gated Ca^{2+} channels (73–75). Here, we demonstrate that the expression of the *P. aeruginosa* TCS CarSR increases in

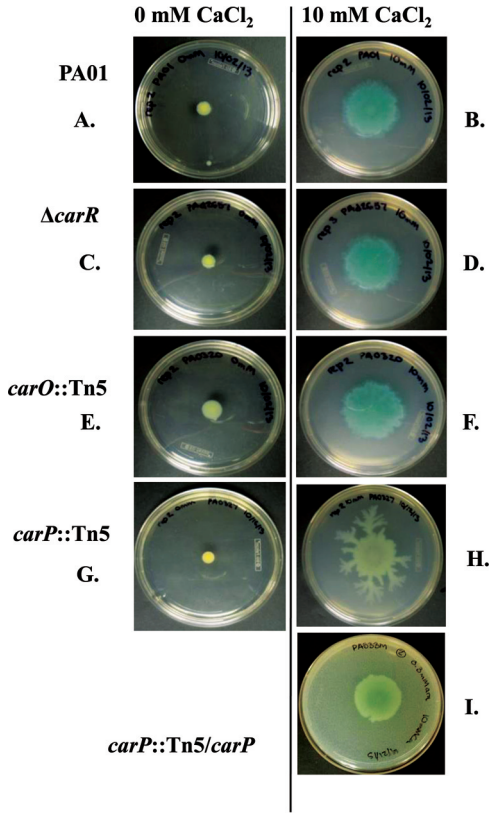

FIG 5 Swarming colonies of *P. aeruginosa* strains growing on BM2 agar with 0 or 10 mM $CaCl_2$. PAO1, Δ*carR*, *carO*::Tn*5*, *carP*::Tn*5*, and *carP*::Tn*5*/*carP* strains were tested. The complemented mutant was grown on BM2 swarm agar containing 10 mM $CaCl_2$ and 0.3 mM arabinose. The diameter and morphology of the colonies were reported after 24 h of incubation. The pictures show representative photographs selected from at least three biological replicates collected from five independent experiments.

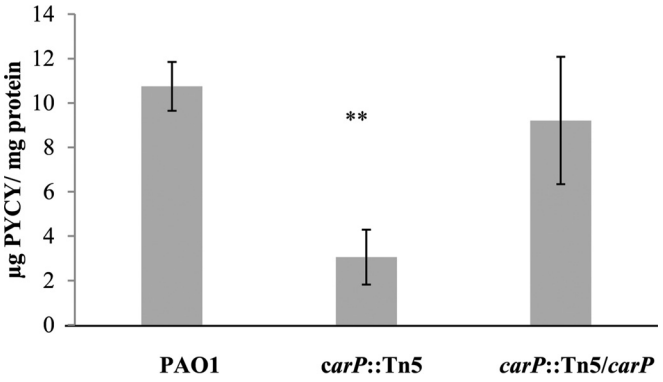

FIG 6 Pyocyanin production by *P. aeruginosa* PAO1, *carP*::Tn*5*, and *carP*::Tn*5*/*carP* strains. Pyocyanin was extracted from swarming colonies grown on BM2 plates in the presence of 10 mM $CaCl_2$. The excised agar plugs containing the colonies were cut into halves. Pyocyanin amounts were quantified from half of the agar plug and then normalized to the total cellular protein extracted from the other half of the plug. The data represent the means and standard deviations for at least three biological replicates in three independent experiments. Statistical significance of the differences was calculated using Student's *t* test. **, $P < 0.005$.

response to high levels of external Ca^{2+}. CarSR in turn regulates the transcription of *carO* and *carP* genes, which are involved in Ca^{2+}-dependent responses. Based on these results, we propose that CarSR is a Ca^{2+}-regulated TCS in *P. aeruginosa* PAO1.

In addition to inducing the transcription of *carSR*, elevated Ca^{2+} represses the transcription of two closely related TCSs, *phoPQ* and *pmrAB*. McPhee showed that *phoPQ* and *pmrAB* also are downregulated by elevated Mg^{2+} (24, 25). Changes in Mg^{2+} concentrations in the media did not affect the transcription of *carSR* (24). The transcriptional response of the TCSs due to Ca^{2+} addition is affected by the mode of growth: expression of *carSR* is induced only in planktonic cultures, whereas expression of *pmrAB* and *phoPQ* is reduced in biofilms and in planktonic cultures. The results suggest an additional level of regulation coordinating responses to Ca^{2+} during a switch from planktonic to biofilm growth.

Comparison of the Ca^{2+}-induced regulon reported here and the Mg^{2+}-induced regulon reported previously (24) revealed that 36 PAO1 genes are positively regulated by elevated Ca^{2+} but not by elevated Mg^{2+}. These genes include PA0102-0104, encoding carbonic anhydrase and permease, hypothetical proteins PA0320 (here named CarO) and PA0327 (here named CarP), which are regulated by *carSR*, and quorum-sensing systems *las* and *rhl*, together with 14 genes regulated by these quorum-sensing proteins (76–78). The latter include *rahU*, involved in modulating biofilm formation and interaction with host innate immunity, *hcnA*, involved in hydrogen cyanide production, *kynB*, involved in the anthranilate pathway, *rhlB*, essential for rhamnolipid biosynthesis, and *pvd* genes, involved in pyoverdine biosynthesis. This comparison found no genes that were significantly induced by elevated levels of both Ca^{2+} and Mg^{2+}. However, 20 genes were downregulated by both cations. Most of these downregulated genes belong to the regulons of PhoPQ and PmrAB, including the *arn* operon (25, 28), which is involved in the modification of LPS with arabinose groups. The *arn*-mediated LPS modifications were shown to increase *P. aeruginosa* resistance to polymyxin B (27). However,

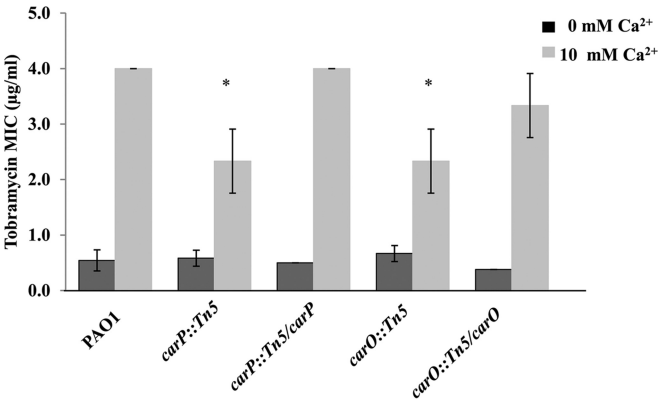

FIG 7 MICs of tobramycin for *P. aeruginosa* PAO1, *carO*::Tn*5*, and *carP*::Tn*5* mutants and their *carO*::Tn*5*-*carO* and *carP*::Tn*5*-*carP* complemented counterparts grown on BMM with 0 mM $CaCl_2$ (dark gray bars) or 10 mM $CaCl_2$ (light gray bars). Cells were grown in BMM without adding $CaCl_2$ until mid-log phase, their OD_{600}s were normalized to 0.1, and aliquots of 100 μl were plated onto BMM agar for MIC measurements. E-strips with tobramycin gradient were placed on the bacterial lawns, and the MICs were recorded after 24 h of incubation. The data represent the means and standard deviations from at least three biological replicates from two independent experiments. The statistical significance of the differences was calculated using Student's *t* test. *, $P < 0.05$.

here we observed a decreased transcription of the *arn* operon and an increase in resistance to polymyxin B in response to elevated Ca^{2+}. This result suggests that *P. aeruginosa* possesses an alternative mechanism for resistance to polymyxin B that is positively regulated by Ca^{2+} and is independent of Arn modification of LPS.

The Ca^{2+}-induced TCS CarSR regulates the expression of *carO* and *carP* in a Ca^{2+}-dependent manner. CarSR, CarO, and CarP all are required for *P. aeruginosa* PAO1 response to elevated Ca^{2+} levels. In particular, CarSR, CarO, and CarP all are required to maintain intracellular $[Ca^{2+}]$ at a low level when cells are grown at low $[Ca^{2+}]$. In addition, CarP is required for maintaining low cytosolic $[Ca^{2+}]$ and for optimal growth when cells are exposed to high $[Ca^{2+}]$. CarP also is involved in other processes that are influenced by high $[Ca^{2+}]$, including modulating the amount of pyocyanin production and affecting swarming motility. Both CarO and CarP also contribute to Ca^{2+}-induced resistance to tobramycin.

The molecular roles of CarO and CarP in Ca^{2+}-dependent processes presently are unknown. Since CarO and CarP are located primarily in the periplasm, they likely are not involved in the direct biosynthesis of pyocyanin, flagella, flagellum motor, or chemotaxis system. However, they may allow the cells to sense or modulate the periplasmic level of Ca^{2+}, which itself plays a role in regulating the production of these factors either directly or via reducing the intracellular concentration of Ca^{2+}. Intracellular $[Ca^{2+}]$ may in turn affect the expression of genes required for pyocyanin production or swarming motility. Whether their activities are direct or indirect, CarO and CarP are important for *P. aeruginosa* responses to high levels of Ca^{2+}, since the phenotypes observed for the *carO* and *carP* mutants occur primarily at high $[Ca^{2+}]$.

The results presented here indicate that the two-component system CarSR is responsible for *P. aeruginosa* sensing elevated levels of external Ca^{2+}, and it is responding through the induction of its regulatory targets, *carO* and *carP*. CarO and CarP affect intracellular Ca^{2+} homeostasis, surface-associated motility, resistance to tobramycin, and the production of the virulence factor pyocyanin.

ACKNOWLEDGMENTS

We thank Jessica Richards for her help with the bioinformatics analysis. We also thank Anthony Campbell from the School of Pharmacy and Pharmaceutical Sciences, Cardiff University, United Kingdom, for sharing his expertise and the templates for calculating $[Ca^{2+}]_{in}$, and Delfina Dominguez from The University of Texas at El Paso for sharing the *E. coli* strain carrying pMMB66EH.

FUNDING INFORMATION

HHS | NIH | National Institute of Allergy and Infectious Diseases (NIAID) provided funding to Michael J. Franklin under grant number AI113330. Oklahoma Center for the Advancement of Science and Technology (OCAST) provided funding to Marianna A. Patrauchan under grant number HR12-167.

REFERENCES

1. **Zhao GJ, Hong GL, Liu JQ, Lu Y, Lu ZQ.** 2014. Septic shock due to community-acquired *Pseudomonas aeruginosa* necrotizing fasciitis: a case report and literature review. Exp Ther Med **7:**1545–1548.
2. **Stover CK, Pham XQ, Erwin AL, Mizoguchi SD, Warrener P, Hickey MJ, Brinkman FS, Hufnagle WO, Kowalik DJ, Lagrou M, Garber RL, Goltry L, Tolentino E, Westbrock-Wadman S, Yuan Y, Brody LL, Coulter SN, Folger KR, Kas A, Larbig K, Lim R, Smith K, Spencer D, Wong GK, Wu Z, Paulsen IT, Reizer J, Saier MH, Hancock RE, Lory S, Olson MV.** 2000. Complete genome sequence of *Pseudomonas aeruginosa* PAO1, an opportunistic pathogen. Nature **406:**959–964. http://dx.doi.org/10.1038/35023079.
3. **Lakkis C, Fleiszig SM.** 2001. Resistance of *Pseudomonas aeruginosa* isolates to hydrogel contact lens disinfection correlates with cytotoxic activity. J Clin Microbiol **39:**1477–1486. http://dx.doi.org/10.1128/JCM.39.4.1477-1486.2001.
4. **Silby MW, Winstanley C, Godfrey SA, Levy SB, Jackson RW.** 2011. Pseudomonas genomes: diverse and adaptable. FEMS Microbiol Rev **35:**652–680. http://dx.doi.org/10.1111/j.1574-6976.2011.00269.x.
5. **Gooderham WJ, Hancock RE.** 2009. Regulation of virulence and antibiotic resistance by two-component regulatory systems in *Pseudomonas aeruginosa*. FEMS Microbiol Rev **33:**279–294. http://dx.doi.org/10.1111/j.1574-6976.2008.00135.x.
6. **Guragain M, Lenaburg DL, Moore FS, Reutlinger I, Patrauchan MA.** 2013. Calcium homeostasis in *Pseudomonas aeruginosa* requires multiple transporters and modulates swarming motility. Cell Calcium **54:**350–361. http://dx.doi.org/10.1016/j.ceca.2013.08.004.
7. **Anderson S, Appanna VD, Huang J, Viswanatha T.** 1992. A novel role for calcite in calcium homeostasis. FEBS Lett **308:**94–96. http://dx.doi.org/10.1016/0014-5793(92)81059-U.
8. **Glunk C, Dupraz C, Braissant O, Gallagher KL, Verrecchia EP, Visscher PT.** 2011. Microbially mediated carbonate precipitation in a hypersaline lake, Big Pond (Eleuthera, Bahamas). Sedimentology **58:**720–738. http://dx.doi.org/10.1111/j.1365-3091.2010.01180.x.
9. **Steinhorst L, Kudla J.** 2013. Calcium–a central regulator of pollen germination and tube growth. Biochim Biophys Acta **1833:**1573–1581. http://dx.doi.org/10.1016/j.bbamcr.2012.10.009.
10. **Bose J, Pottosin II, Shabala SS, Palmgren MG, Shabala S.** 2011. Calcium efflux systems in stress signaling and adaptation in plants. Front Plant Sci **2:**85.
11. **Robertson WG, Marshall RW, Bowers GN.** 1981. Ionized calcium in body-fluids. Crit Rev Clin Lab Sci **15:**85–125. http://dx.doi.org/10.3109/10408368109105869.
12. **Blomfiel J, Warton KL, Brown JM.** 1973. Flow-rate and inorganic components of submandibular saliva in cystic-fibrosis. Arch Dis Childhood **48:**267–274. http://dx.doi.org/10.1136/adc.48.4.267.
13. **Berg JM, Tymoczko JL, Stryer L.** 2002. Biochemistry, vol 5. WH Freeman & Co, New York, NY.
14. **Vitolo MR, Valente Soares LM, Carvalho EB, Cardoso CB.** 2004. Calcium and magnesium concentrations in mature human milk: influence of calcium intake, age and socioeconomic level. Arch Latinoam Nutr **54:**118–122.
15. **Halmerbauer G, Arri S, Schierl M, Strauch E, Koller DY.** 2000. The relationship of eosinophil granule proteins to ions in the sputum of patients with cystic fibrosis. Clin Exp Allergy **30:**1771–1776. http://dx.doi.org/10.1046/j.1365-2222.2000.00988.x.
16. **Lorin MI, Gaerlan PF, Mandel ID, Denning CR.** 1976. Composition of nasal secretion in patients with cystic-fibrosis. J Lab Clin Med **88:**114–117.
17. **Sanders NN, Franckx H, De Boeck K, Haustraete J, De Smedt SC, Demeester J.** 2006. Role of magnesium in the failure of rhDNase therapy in patients with cystic fibrosis. Thorax **61:**962–968. http://dx.doi.org/10.1136/thx.2006.060814.
18. **Smith DJ, Anderson GJ, Bell SC, Reid DW.** 2014. Elevated metal concentrations in the CF airway correlate with cellular injury and disease severity. J Cyst Fibros **13:**289–295. http://dx.doi.org/10.1016/j.jcf.2013.12.001.
19. **Sarkisova S, Patrauchan MA, Berglund D, Nivens DE, Franklin MJ.** 2005. Calcium-induced virulence factors associated with the extracellular matrix of mucoid *Pseudomonas aeruginosa* biofilms. J Bacteriol **187:**4327–4337. http://dx.doi.org/10.1128/JB.187.13.4327-4337.2005.
20. **Patrauchan MA, Sarkisova SA, Franklin MJ.** 2007. Strain-specific proteome responses of *Pseudomonas aeruginosa* to biofilm-associated growth and to calcium. Microbiology **153:**3838–3851. http://dx.doi.org/10.1099/mic.0.2007/010371-0.
21. **Sarkisova SA, Lotlikar SR, Guragain M, Kubat R, Cloud J, Franklin MJ, Patrauchan MA.** 2014. A *Pseudomonas aeruginosa* EF-hand protein, EfhP (PA4107), modulates stress responses and virulence at high calcium concentration. PLoS One **9:**e98985. http://dx.doi.org/10.1371/journal.pone.0098985.
22. **Stock AM, Robinson VL, Goudreau PN.** 2000. Two-component signal

transduction. Annu Rev Biochem **69:**183–215. http://dx.doi.org/10.1146/annurev.biochem.69.1.183.
23. **Hoch JA.** 2000. Two-component and phosphorelay signal transduction. Curr Opin Microbiol **3:**165–170. http://dx.doi.org/10.1016/S1369-5274(00)00070-9.
24. **McPhee JB, Bains M, Winsor G, Lewenza S, Kwasnicka A, Brazas MD, Brinkman FS, Hancock RE.** 2006. Contribution of the PhoP-PhoQ and PmrA-PmrB two-component regulatory systems to Mg^{2+}-induced gene regulation in *Pseudomonas aeruginosa*. J Bacteriol **188:**3995–4006. http://dx.doi.org/10.1128/JB.00053-06.
25. **McPhee JB, Lewenza S, Hancock REW.** 2003. Cationic antimicrobial peptides activate a two-component regulatory system, PmrA-PmrB, that regulates resistance to polymyxin B and cationic antimicrobial peptides in *Pseudomonas aeruginosa*. Mol Microbiol **50:**205–217. http://dx.doi.org/10.1046/j.1365-2958.2003.03673.x.
26. **Moskowitz SM, Ernst RK, Miller SI.** 2004. PmrAB, a two-component regulatory system of *Pseudomonas aeruginosa* that modulates resistance to cationic antimicrobial peptides and addition of aminoarabinose to lipid A. J Bacteriol **186:**575–579. http://dx.doi.org/10.1128/JB.186.2.575-579.2004.
27. **Miller AK, Brannon MK, Stevens L, Johansen HK, Selgrade SE, Miller SI, Hoiby N, Moskowitz SM.** 2011. PhoQ mutations promote lipid A modification and polymyxin resistance of *Pseudomonas aeruginosa* found in colistin-treated cystic fibrosis patients. Antimicrob Agents Chemother **55:**5761–5769. http://dx.doi.org/10.1128/AAC.05391-11.
28. **Gooderham WJ, Gellatly SL, Sanschagrin F, McPhee JB, Bains M, Cosseau C, Levesque RC, Hancock RE.** 2009. The sensor kinase PhoQ mediates virulence in *Pseudomonas aeruginosa*. Microbiology **155:**699–711. http://dx.doi.org/10.1099/mic.0.024554-0.
29. **Brinkman FSL, MacFarlane ELA, Warrener P, Hancock REW.** 2001. Evolutionary relationships among virulence-associated histidine kinases. Infect Immun **69:**5207–5211. http://dx.doi.org/10.1128/IAI.69.8.5207-5211.2001.
30. **Kwon DH, Lu CD.** 2006. Polyamines induce resistance to cationic peptide, aminoglycoside, and quinolone antibiotics in *Pseudomonas aeruginosa* PAO1. Antimicrob Agents Chemother **50:**1615–1622. http://dx.doi.org/10.1128/AAC.50.5.1615-1622.2006.
31. **Perron K, Caille O, Rossier C, van Delden C, Dumas JL, Kohler T.** 2004. CzcR-CzcS, a two-component system involved in heavy metal and carbapenem resistance in *Pseudomonas aeruginosa*. J Biol Chem **279:**8761–8768. http://dx.doi.org/10.1074/jbc.M312080200.
32. **Teitzel GM, Geddie A, De Long SK, Kirisits MJ, Whiteley M, Parsek MR.** 2006. Survival and growth in the presence of elevated copper: transcriptional profiling of copper-stressed *Pseudomonas aeruginosa*. J Bacteriol **188:**7242–7256. http://dx.doi.org/10.1128/JB.00837-06.
33. **Rahme LG, Ausubel FM, Cao H, Drenkard E, Goumnerov BC, Lau GW, Mahajan-Miklos S, Plotnikova J, Tan MW, Tsongalis J, Walendziewicz CL, Tompkins RG.** 2000. Plants and animals share functionally common bacterial virulence factors. Proc Natl Acad Sci U S A **97:**8815–8821. http://dx.doi.org/10.1073/pnas.97.16.8815.
34. **Overhage J, Lewenza S, Marr AK, Hancock RE.** 2007. Identification of genes involved in swarming motility using a *Pseudomonas aeruginosa* PAO1 mini-Tn5-lux mutant library. J Bacteriol **189:**2164–2169. http://dx.doi.org/10.1128/JB.01623-06.
35. **Whitchurch CB, Alm RA, Mattick JS.** 1996. The alginate regulator AlgR and an associated sensor FimS are required for twitching motility in *Pseudomonas aeruginosa*. Proc Natl Acad Sci U S A **93:**9839–9843. http://dx.doi.org/10.1073/pnas.93.18.9839.
36. **Carterson AJ, Morici LA, Jackson DW, Frisk A, Lizewski SE, Jupiter R, Simpson K, Kunz DA, Davis SH, Schurr JR, Hassett DJ, Schurr MJ.** 2004. The transcriptional regulator AlgR controls cyanide production in *Pseudomonas aeruginosa*. J Bacteriol **186:**6837–6844. http://dx.doi.org/10.1128/JB.186.20.6837-6844.2004.
37. **Lizewski SE, Lundberg DS, Schurr MJ.** 2002. The transcriptional regulator AlgR is essential for *Pseudomonas aeruginosa* pathogenesis. Infect Immun **70:**6083–6093. http://dx.doi.org/10.1128/IAI.70.11.6083-6093.2002.
38. **Reimmann C, Beyeler M, Latifi A, Winteler H, Foglino M, Lazdunski A, Haas D.** 1997. The global activator GacA of *Pseudomonas aeruginosa* PAO positively controls the production of the autoinducer N-butyryl-homoserine lactone and the formation of the virulence factors pyocyanin, cyanide, and lipase. Mol Microbiol **24:**309–319. http://dx.doi.org/10.1046/j.1365-2958.1997.3291701.x.
39. **Linares JF, Gustafsson I, Baquero F, Martinez JL.** 2006. Antibiotics as intermicrobial signaling agents instead of weapons. Proc Natl Acad Sci U S A **103:**19484–19489. http://dx.doi.org/10.1073/pnas.0608949103.
40. **Whitchurch CB, Erova TE, Emery JA, Sargent JL, Harris JM, Semmler ABT, Young MD, Mattick JS, Wozniak DJ.** 2002. Phosphorylation of the *Pseudomonas aeruginosa* response regulator AlgR is essential for type IV fimbria-mediated twitching motility. J Bacteriol **184:**4544–4554. http://dx.doi.org/10.1128/JB.184.16.4544-4554.2002.
41. **Morici LA, Carterson AJ, Wagner VE, Frisk A, Schurr JR, Bentrup KHZ, Hassett DJ, Iglewski BH, Sauer K, Schurr MJ.** 2007. *Pseudomonas aeruginosa* AlgR represses the Rhl quorum-sensing system in a biofilm-specific manner. J Bacteriol **189:**7752–7764. http://dx.doi.org/10.1128/JB.01797-06.
42. **Ritchings BW, Almira EC, Lory S, Ramphal R.** 1995. Cloning and phenotypic characterization of Fles and Fler, new response regulators of Pseudomonas aeruginosa which regulate motility and adhesion to mucin. Infect Immun **63:**4868–4876.
43. **Breidenstein EBM, Khaira BK, Wiegand I, Overhage J, Hancock REW.** 2008. Complex ciprofloxacin resistome revealed by screening a *Pseudomonas aeruginosa* mutant library for altered susceptibility. Antimicrob Agents Chemother **52:**4486–4491. http://dx.doi.org/10.1128/AAC.00222-08.
44. **Hurley BP, Goodman AL, Mumy KL, Murphy P, Lory S, McCormick BA.** 2010. The two-component sensor response regulator RoxS/RoxR plays a role in *Pseudomonas aeruginosa* interactions with airway epithelial cells. Microbes Infect **12:**190–198. http://dx.doi.org/10.1016/j.micinf.2009.11.009.
45. **Silo-Suh LA, Suh SJ, Ohman DE, Wozniak DJ, Pridgeon JW.** 2015. Complete genome sequence of *Pseudomonas aeruginosa* mucoid strain FRD1, isolated from a cystic fibrosis patient. Genome Announc **3:**e00153-15.
46. **Damron FH, McKenney ES, Schweizer HP, Goldberg JB.** 2013. Construction of a broad-host-range Tn7-based vector for single-copy PBAD-controlled gene expression in Gram-negative bacteria. Appl Environ Microbiol **79:**718–721. http://dx.doi.org/10.1128/AEM.02926-12.
47. **Hoang TT, Karkhoff-Schweizer RR, Kutchma AJ, Schweizer HP.** 1998. A broad-host-range Flp-FRT recombination system for site-specific excision of chromosomally-located DNA sequences: application for isolation of unmarked *Pseudomonas aeruginosa* mutants. Gene **212:**77–86. http://dx.doi.org/10.1016/S0378-1119(98)00130-9.
48. **Watkins NJ, Knight MR, Trewavas AJ, Campbell AK.** 1995. Free calcium transients in chemotactic and non-chemotactic strains of Escherichia coli determined by using recombinant aequorin. Biochem J **306:**865–869.
49. **Irani VR, Rowe JJ.** 1997. Enhancement of transformation in *Pseudomonas aeruginosa* PAO1 by Mg2+ and heat. Biotechniques **22:**54–56.
50. **Lenz AP, Williamson KS, Pitts B, Stewart PS, Franklin MJ.** 2008. Localized gene expression in *Pseudomonas aeruginosa* biofilms. Appl Environ Microbiol **74:**4463–4471. http://dx.doi.org/10.1128/AEM.00710-08.
51. **Stewart PS, Franklin MJ, Williamson KS, Folsom JP, Boegli L, James GA.** 2015. Contribution of stress responses to antibiotic tolerance in *Pseudomonas aeruginosa* biofilms. Antimicrob Agents Chemother **59:**3838–3847. http://dx.doi.org/10.1128/AAC.00433-15.
52. **Williamson KS, Richards LA, Perez-Osorio AC, Pitts B, McInnerney K, Stewart PS, Franklin MJ.** 2012. Heterogeneity in *Pseudomonas aeruginosa* biofilms includes expression of ribosome hibernation factors in the antibiotic-tolerant subpopulation and hypoxia-induced stress response in the metabolically active population. J Bacteriol **194:**2062–2073. http://dx.doi.org/10.1128/JB.00022-12.
53. **Pfaffl MW, Horgan GW, Dempfle L.** 2002. Relative expression software tool (REST) for group-wise comparison and statistical analysis of relative expression results in real-time PCR. Nucleic Acids Res **30:**e36. http://dx.doi.org/10.1093/nar/30.9.e36.
54. **Jones HE, Holland IB, Baker HL, Campbell AK.** 1999. Slow changes in cytosolic free Ca2+ in *Escherichia coli* highlight two putative influx mechanisms in response to changes in extracellular calcium. Cell Calcium **25:**265–274. http://dx.doi.org/10.1054/ceca.1999.0028.
55. **Kurachi M.** 1958. Studies on the biosynthesis of pyocyanine. (II) Isolation and determination of pyocyanin. Bull Inst Chem Res Kyoto Univ **36:**13.
56. **Tamura K, Dudley J, Nei M, Kumar S.** 2007. MEGA4: Molecular Evolutionary Genetics Analysis (MEGA) software version 4.0. Mol Biol Evol **24:**1596–1599. http://dx.doi.org/10.1093/molbev/msm092.
57. **Punta M, Coggill PC, Eberhardt RY, Mistry J, Tate J, Boursnell C, Pang N, Forslund K, Ceric G, Clements J, Heger A, Holm L, Sonnhammer**

EL, Eddy SR, Bateman A, Finn RD. 2012. The Pfam protein families database. Nucleic Acids Res **40:**D290–D301. http://dx.doi.org/10.1093/nar/gkr1065.
58. **Yu NY, Wagner JR, Laird MR, Melli G, Rey S, Lo R, Dao P, Sahinalp SC, Ester M, Foster LJ, Brinkman FS.** 2010. PSORTb 3.0: improved protein subcellular localization prediction with refined localization subcategories and predictive capabilities for all prokaryotes. Bioinformatics **26:**1608–1615. http://dx.doi.org/10.1093/bioinformatics/btq249.
59. **Nair R, Rost B.** 2005. Mimicking cellular sorting improves prediction of subcellular localization. J Mol Biol **348:**85–100. http://dx.doi.org/10.1016/j.jmb.2005.02.025.
60. **Moller S, Croning MD, Apweiler R.** 2001. Evaluation of methods for the prediction of membrane spanning regions. Bioinformatics **17:**646–653. http://dx.doi.org/10.1093/bioinformatics/17.7.646.
61. **Petersen TN, Brunak S, von Heijne G, Nielsen H.** 2011. SignalP 4.0: discriminating signal peptides from transmembrane regions. Nat Methods **8:**785–786. http://dx.doi.org/10.1038/nmeth.1701.
62. **Biegert A, Mayer C, Remmert M, Söding J, Lupas AN.** 2006. The MPI Bioinformatics Toolkit for protein sequence analysis. Nucleic Acids Res **34:**W335–W339. http://dx.doi.org/10.1093/nar/gkl217.
63. **Yang J, Yan R, Roy A, Xu D, Poisson J, Zhang Y.** 2015. The I-TASSER Suite: protein structure and function prediction. Nat Methods **12:**7–8.
64. **Edgar R, Domrachev M, Lash AE.** 2002. Gene Expression Omnibus: NCBI gene expression and hybridization array data repository. Nucleic Acids Res **30:**207–210. http://dx.doi.org/10.1093/nar/30.1.207.
65. **Macfarlane EL, Kwasnicka A, Ochs MM, Hancock RE.** 1999. PhoP-PhoQ homologues in *Pseudomonas aeruginosa* regulate expression of the outer-membrane protein OprH and polymyxin B resistance. Mol Microbiol **34:**305–316. http://dx.doi.org/10.1046/j.1365-2958.1999.01600.x.
66. **Fukushima K, Kumar SD, Suzuki S.** 2012. YgiW homologous gene from *Pseudomonas aeruginosa* 25W is responsible for tributyltin resistance. J Gen Appl Microbiol **58:**283–289. http://dx.doi.org/10.2323/jgam.58.283.
67. **Lee J, Hiibel SR, Reardon KF, Wood TK.** 2010. Identification of stress-related proteins in *Escherichia coli* using the pollutant cis-dichloroethylene. J Appl Microbiol **108:**2088–2102.
68. **Chen CK, Chan NL, Wang AH.** 2011. The many blades of the beta-propeller proteins: conserved but versatile. Trends Biochem Sci **36:**553–561. http://dx.doi.org/10.1016/j.tibs.2011.07.004.
69. **Jacobs MA, Alwood A, Thaipisuttikul I, Spencer D, Haugen E, Ernst S, Will O, Kaul R, Raymond C, Levy R, Chun-Rong L, Guenthner D, Bovee D, Olson MV, Manoil C.** 2003. Comprehensive transposon mutant library of *Pseudomonas aeruginosa*. Proc Natl Acad Sci U S A **100:**14339–14344. http://dx.doi.org/10.1073/pnas.2036282100.
70. **Prost LR, Miller SI.** 2008. The Salmonellae PhoQ sensor: mechanisms of detection of phagosome signals. Cell Microbiol **10:**576–582. http://dx.doi.org/10.1111/j.1462-5822.2007.01111.x.
71. **Vescovi EG, Ayala YM, Di Cera E, Groisman EA.** 1997. Characterization of the bacterial sensor protein PhoQ. Evidence for distinct binding sites for Mg2+ and Ca2+. J Biol Chem **272:**1440–1443.
72. **Bilecen K, Yildiz FH.** 2009. Identification of a calcium-controlled negative regulatory system affecting *Vibrio cholerae* biofilm formation. Environ Microbiol **11:**2015–2029. http://dx.doi.org/10.1111/j.1462-2920.2009.01923.x.
73. **Theodorou MC, Panagiotidis CA, Panagiotidis CH, Pantazaki AA, Kyriakidis DA.** 2006. Involvement of the AtoS-AtoC signal transduction system in poly-(R)-3-hydroxybutyrate biosynthesis in *Escherichia coli*. Biochim Biophys Acta **1760:**896–906. http://dx.doi.org/10.1016/j.bbagen.2006.01.020.
74. **Reusch RN, Huang R, Bramble LL.** 1995. Poly-3-hydroxybutyrate/polyphosphate complexes form voltage-activated Ca2+ channels in the plasma membranes of *Escherichia coli*. Biophys J **69:**754–766. http://dx.doi.org/10.1016/S0006-3495(95)79958-1.
75. **Theodorou MC, Tiligada E, Kyriakidis DA.** 2009. Extracellular Ca2+ transients affect poly-(R)-3-hydroxybutyrate regulation by the AtoS-AtoC system in *Escherichia coli*. Biochem J **417:**667–672. http://dx.doi.org/10.1042/BJ20081169.
76. **Wagner VE, Bushnell D, Passador L, Brooks AI, Iglewski BH.** 2003. Microarray analysis of *Pseudomonas aeruginosa* quorum-sensing regulons: effects of growth phase and environment. J Bacteriol **185:**2080–2095. http://dx.doi.org/10.1128/JB.185.7.2080-2095.2003.
77. **Schuster M, Lostroh CP, Ogi T, Greenberg E.** 2003. Identification, timing, and signal specificity of *Pseudomonas aeruginosa* quorum-controlled genes: a transcriptome analysis. J Bacteriol **185:**2066–2079. http://dx.doi.org/10.1128/JB.185.7.2066-2079.2003.
78. **Bredenbruch F, Geffers R, Nimtz M, Buer J, Häussler S.** 2006. The *Pseudomonas aeruginosa* quinolone signal (PQS) has an iron-chelating activity. Environ Microbiol **8:**1318–1329. http://dx.doi.org/10.1111/j.1462-2920.2006.01025.x.